Carbon monoxide measured by the EOS Microwave Limb Sounder on Aura: First results

Mark J. Filipiak,[1] Robert S. Harwood,[1] Jonathan H. Jiang,[2] Qinbin Li,[2] Nathaniel J. Livesey,[2] Gloria L. Manney,[2,3] William G. Read,[2] Michael J. Schwartz,[2] Joe W. Waters,[2] and Dong L. Wu[2]

Received 21 February 2005; revised 14 May 2005; accepted 19 May 2005; published 28 July 2005.

[1] Atmospheric carbon monoxide (CO) is measured by the EOS Microwave Limb Sounder (MLS) on NASA's recently-launched Aura satellite. Descent has been observed in the 2004–2005 Northern Hemisphere winter polar mesosphere and upper stratosphere. During August and September 2004 enhanced CO was observed in the upper troposphere over India and Tibet. The MLS CO measurements are described and the radiance signal due to the enhanced CO in the upper troposphere is demonstrated.
Citation: Filipiak, M. J., R. S. Harwood, J. H. Jiang, Q. Li, N. J. Livesey, G. L. Manney, W. G. Read, M. J. Schwartz, J. W. Waters, and D. L. Wu (2005), Carbon monoxide measured by the EOS Microwave Limb Sounder on Aura: First results, *Geophys. Res. Lett.*, *32*, L14825, doi:10.1029/2005GL022765.

1. Introduction

[2] The Earth Observing System Microwave Limb Sounder (EOS MLS) launched on NASA's Aura satellite in July 2004 is making continuous global measurements of carbon monoxide (CO) from the upper troposphere to the lower thermosphere.

[3] In the troposphere, CO is a product of incomplete combustion of fossil-fuel and biomass and is present at concentrations of 50–500 ppbv. It is the principal sink of the hydroxyl radical (OH), which is the main tropospheric oxidant. CO has a photochemical lifetime of about two months in the troposphere and is therefore a sensitive tracer for transport of continental boundary layer pollution. Deep convection can lift polluted boundary layer air into the upper troposphere [e.g., *Kar et al.*, 2004] where it can be advected over long distances by upper-level winds.

[4] In the upper atmosphere, the dominant source of CO is photolysis of carbon dioxide in the thermosphere and the only sink is oxidation by OH. The loss rate in the thermosphere is negligible, so CO increases rapidly with altitude. The photochemical lifetime of CO is 1–3 months in the mesosphere and stratosphere, longer than the time-scale for vertical transport at these altitudes, which makes it a tracer of transport [*Allen et al.*, 1999]. In the winter polar night, CO is conserved and becomes an excellent tracer of vertical transport in the polar vortex.

[5] This paper presents first results of CO measurements from EOS MLS on Aura. We concentrate on showing the radiance spectral signatures that are the basis for the CO measurements (especially upper tropospheric CO which is one of the more challenging measurements for EOS MLS), and on showing results regarding the use of CO as a tracer, where accurate absolute magnitudes are less important. Determination of the absolute accuracies of the MLS CO measurements are now underway as part of extensive Aura validation activities and will be documented later; we currently estimate 10% for the absolute accuracy, based on absolute accuracies in instrument calibration and spectroscopy data.

2. The EOS MLS Instrument and Data

[6] MLS measures the thermal emission lines of trace gases, at frequencies ranging from 118 GHz to 2.5 THz [*Waters et al.*, 1999]. MLS looks forward along the Aura orbit. Its antenna is pointed so that its beam is tangential to the Earth's surface, and moved to scan the narrow (~3 km in the vertical at the tangent point at the frequencies used to measure CO) field-of-view through the atmosphere from the ground to 100 km. It performs one scan every 1.5° of the Aura orbit.

[7] CO is measured from its $J = 2 \rightarrow 1$ rotational transition at 230.538 GHz. Three spectrometers are targeted at this line. A 25-channel (resolution 6–96 MHz) filter bank (total width 1.2 GHz), resolves the pressure broadened line in the stratosphere and upper troposphere. A digital autocorrelator spectrometer (129 channels, resolution ~0.1 MHz) resolves the narrow (~1 MHz) Doppler broadened line in the mesosphere and upper stratosphere. A set of 4 wide-band (500 MHz) filters measures background radiance in the upper troposphere. MLS is a double side-band receiver so it simultaneously receives ~230 and ~249 GHz signals in these spectrometers. Figure 1 shows calibrated radiance spectra for the CO line, measured on 30 August 2004, averaged over the latitude and height bins indicated. The marked north-south asymmetry in Figure 1b (and the center channels in Figure 1a) is due to descent of CO-rich air into the winter (south) polar stratosphere and mesosphere and ascent of CO-poor air into the summer (north) polar mesosphere. There are strong ozone lines at the edges of the filter bank passband and several weak ozone and nitric acid lines throughout the passband.

[8] The radiance measurements are transformed to mixing ratios by inverting a forward model using optimal

[1]Institute of Atmospheric and Environmental Science, School of GeoSciences, University of Edinburgh, Edinburgh, UK.
[2]Jet Propulsion Laboratory, California Institute of Technology, Pasadena, California, USA.
[3]Also at Department of Natural Sciences, New Mexico Highlands University, New Mexico, USA.

0094-8276/05/2005GL022765

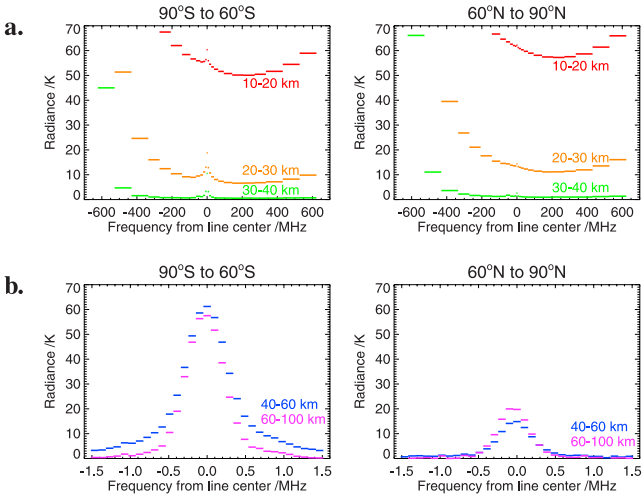

Figure 1. Radiance spectra measured by EOS MLS on 30 August 2004. Each spectrum is centered on the 230 GHz CO emission line and is an average over the latitude and height ranges shown. Each channel is plotted as a horizontal bar with width equal to the nominal bandwidth of the channel. (a) Spectra for the filter bank (Band 9); channels vary in bandwidth from 96 MHz at the wings to 6 MHz at line center. (b) Spectra for the digital autocorrelator spectrometer (Band 25); only the center 31 channels shown; channels have 0.1 MHz bandwidth.

estimation (W. G. Read et al., The clear-sky unpolarized forward model for the EOS Microwave Limb Sounder (MLS); M. J. Schwartz et al., Polarized radiative transfer for Zeeman-split oxygen lines in the EOS MLS forward model; N. J. Livesey et al., Retrieval algorithms for the EOS Microwave Limb Sounder (MLS) instrument; all submitted to *IEEE Transactions on Geoscience and Remote Sensing*, 2005 for the Aura special issue). The inversion (retrieval) algorithm for CO includes the major interfering species (ozone, water vapor, nitric acid) and retrieves these together with temperature, using several frequency bands. Radiance noise transforms to uncertainty in the retrieved CO; the uncertainty for individual profile retrievals ranges from ~30 ppbv in the upper troposphere and lower stratosphere to 0.3–3 ppmv in the mesosphere, and can be reduced by averaging data. The vertical resolution of the CO measurements is ~4 km and the horizontal resolution ~3° along the orbit. The CO results shown here are from MLS Version 1.5 data, the first version being made publicly available.

[9] A tomographic retrieval is performed, giving a continuous slice of measurements through the atmosphere. Two orbits of this slice for CO in the mesosphere and upper stratosphere are shown in Figure 2, one orbit from a late southern winter day, the other for a late northern winter day. In each case descent of CO rich air from the lower thermosphere can be clearly seen in the winter vortex, along with large scale horizontal structures.

[10] The data have been subject to initial validation. This consists of comparing the data with climatology, and comparing radiance calculated from the data with the measured radiance. The radiance fit is generally within the expected calibration and modelling uncertainties and the scatter matches the radiance noise, indicating that the retrieval is consistent with the measured radiances. Demonstration that the signal from the retrieved CO is evident in the measured radiances, as done here, is an important aspect of initial validation. The measured CO mixing ratios are generally higher than climatology in the upper mesosphere and in the troposphere at 215 hPa. Results from an initial comparison of EOS MLS against other satellite data sets will be reported in a future paper (L. Froideveaux et al., Early validation analyses of atmospheric profiles from EOS MLS on the Aura satellite, submitted to *IEEE Transactions on Geoscience and Remote Sensing*, 2005 for the Aura special issue).

3. CO in the Stratosphere and Mesosphere: Dynamics of the Polar Vortex

[11] During the polar winter, descent in the vortex brings carbon monoxide rich air from the thermosphere and mesosphere into the stratosphere [*Allen et al.*, 1999]. In the winter polar night there is no OH in the stratosphere and lower

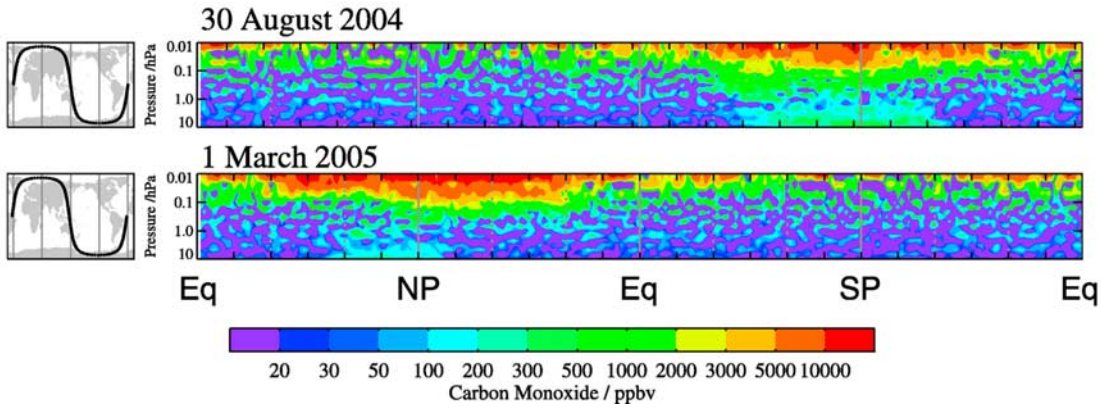

Figure 2. Carbon monoxide in the mesosphere and upper stratosphere measured by MLS in (top) late southern winter and (bottom) late northern winter. Each panel is for one orbit out of the 14 made per day. The orbit track can be seen on the maps on the left (Aura moves along this track from right to left in this view). The speckle is measurement noise.

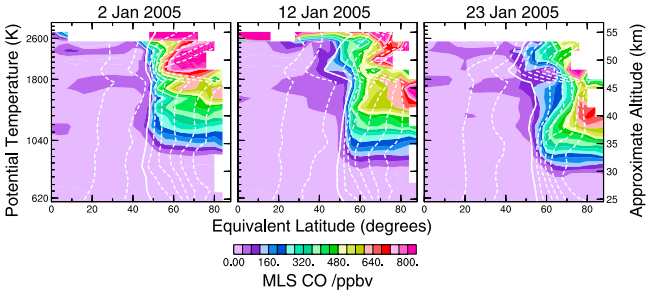

Figure 3. Equivalent latitude/potential temperature averaged cross-sections of CO in the lower mesosphere and upper stratosphere, for the Northern Hemisphere during the NH winter 2004–2005. White curves are contours of potential vorticity (scaled to have a similar range of values throughout the stratosphere [*Manney et al.*, 1999]), the solid contour is a value in the region of the polar vortex edge in the stratosphere. Potential vorticity is taken from the GMAO GEOS-4 assimilation.

mesosphere to destroy the CO, so it acts as a good tracer of vortex dynamics until spring. MLS CO measurements have been averaged and put onto equivalent-latitude/potential temperature coordinates [*Manney et al.*, 1999] (Figure 3) to follow the dynamics of the late 2004–2005 NH polar vortex. (The equivalent latitude of a point is the latitude circle which encloses the same area as the potential vorticity (PV) contour on which the point lies.) Descent in the upper stratosphere can be clearly seen in the time sequence of plots, with descent rates approaching 21K/day in the upper stratosphere. The descending CO-rich air reaches ~28 km during the 2004–2005 northern winter.

[12] However, as shown in Figure 4, the vortex is often distorted/displaced so that large regions are in sunlight and, as seen in the 12 January 2005 map, planetary wave activity can pull filaments of vortex air off into mid-latitudes. While the region of enhanced CO correlates well with the vortex, inhomogeneities within the vortex (such as on 23 January) do not always correspond closely to dynamical variations as seen in PV. This may be due to chemical loss from OH in sunlit regions, to mixing on scales not apparent in the PV contours, or to inaccuracies in the PV field at this level

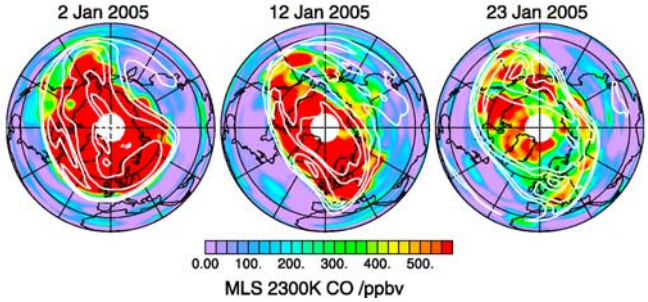

Figure 4. CO in the NH mesosphere during winter 2004–2005. White curves are contours of potential vorticity defining the edge of the winter polar vortex. The θ = 2300K level is at approximately 0.464 hPa ~58 km.

where the meteorological analyses are not well constrained by observations.

4. CO in the Troposphere: Convection of Polluted Boundary Layer Air Into the Upper Troposphere

[13] Carbon monoxide can be transported from the boundary layer (BL) into the upper troposphere by frontal lifting, deep convection, and orographic lifting. MLS observed a strong enhancement in CO in the upper troposphere over southern Asia during 25 August to 6 September 2004, with the maximum occurring on 30 August 2004 (Figure 5), reaching 180 ppbv. *Li et al.* [2005] compare the MLS observations of this enhanced CO with observations by the MOPITT (Measurements Of Pollution In The Troposphere) instrument and with the GEOS-CHEM model. The MOPITT observations of CO at 150 hPa averaged over the same period show a similar enhancement (although MOPITT has missing data over much of the area of enhanced CO, due to the presence of clouds). The modelling studies show that the enhanced CO is polluted BL air transported into the upper troposphere by the Asian monsoon circulation, then trapped in the upper-level anticyclone to the east of Tibet, as well as transported in the tropical easterly jet to the Arabian Sea.

[14] The enhanced CO signal is clearly seen in the measured radiances, once the contributions from water vapor and ozone are removed. Figure 6a shows the measured radiances for the filter bank (Band 9) for 30 August 2004 at a tangent pressure of 147 hPa, averaged over two regions: the tropical Pacific (25S to 25N, 150E to 90W, excluding North America), a region with low mixing ratios of CO in the upper troposphere (confirmed in the MLS measurements); and the region in centered on the CO enhancement (10N to 30N, 50E to 120E). The difference between the two is dominated by differences in the spectrally flat (over the bandwidth used for CO) radiance from the water vapor and dry-air (oxygen and nitrogen) continua,

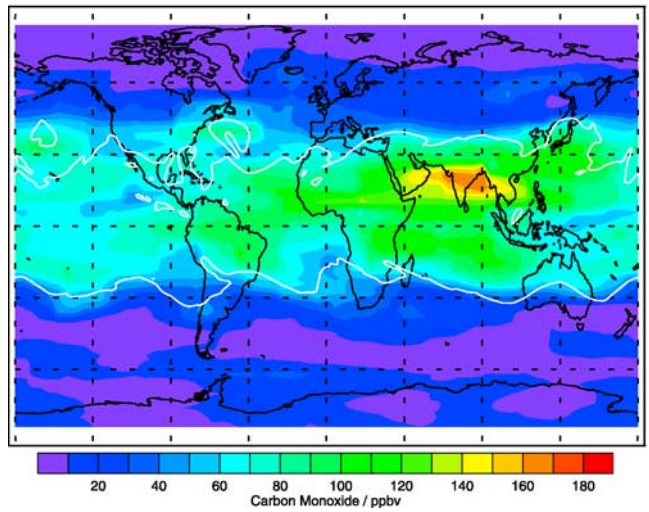

Figure 5. CO measured by MLS at 147 hPa (upper troposphere in the tropics, lower stratosphere at mid- and high-latitudes) for 30 August 2004. White curves are contours of potential vorticity ($\pm 2.0 \times 10^{-6}$K m^2 kg^{-1} s^{-1}) defining the dynamical tropopause.

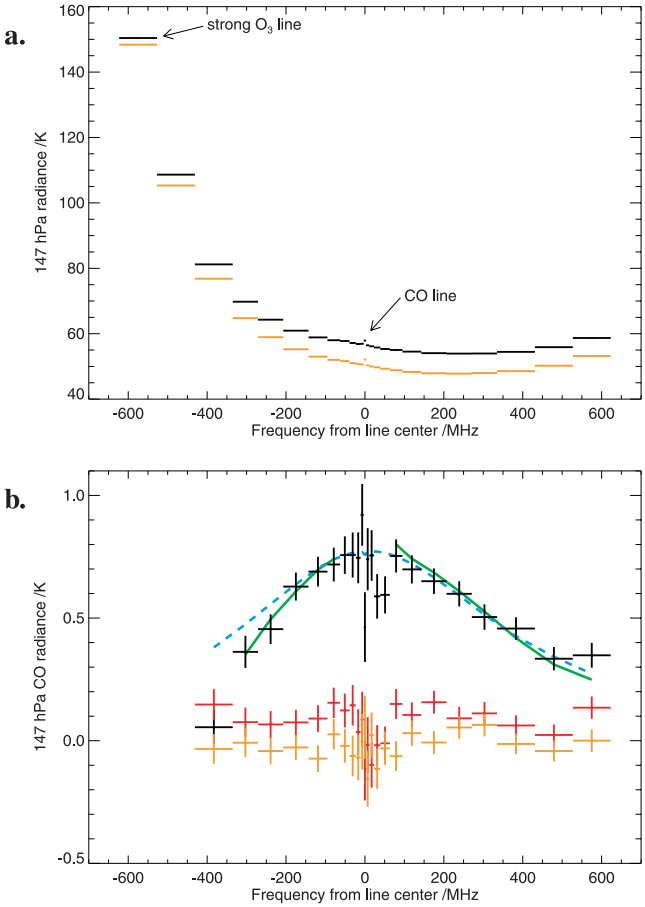

Figure 6. Radiance spectra for Band 9 measured by MLS on 30 August 2004. The radiance for each channel is plotted as a horizontal bar with width equal to the nominal bandwidth of the channel. (a) Measured radiance averaged over the tropical Pacific (orange lines) and south Asia (black lines). (b) Radiance difference between south Asia and tropical Pacific, with the contributions from water vapor, dry-air, and ozone removed. Black crosses are the measured radiance difference (the averaged radiance noise is plotted as the vertical bar), green line is the radiance difference calculated from the retrieved geophysical parameters, and the blue dashed line is calculated relative sensitivity of radiance at 147 hPa to CO at 147 hPa. The two wing channels affected most by the strong ozone line are not plotted; these channels are not used in the CO retrievals. Red and orange crosses are similar radiance differences between north and south, and east and west tropical Pacific regions.

and by differences in the spectrally varying ozone radiance. The continuum radiance is removed by subtracting the radiance in a window channel (Band 33 channel 3, at ~231.8 GHz in the lower side-band, ~247.4 GHz in the upper side-band). The spectrally varying ozone radiance contribution is removed as follows. A channel (Band 7 channel 25, at ~236.3 GHz/243.1 GHz) is chosen which is sensitive to ozone in the upper troposphere but not to CO, and only weakly sensitive to stratospheric ozone. Then, for the Pacific region, a weighted least squares linear fit is calculated for each channel of Band 9 against the radiance in this 'ozone only' channel. The coefficients of the fit are then used in the south Asian region to estimate Band 9 radiances from the Band 7 channel 25 radiances. Figure 6b shows the residual radiance averaged over the south Asian region after removing these two contributions. There is a clear spectral signal centered on the CO line. The signal matches that expected from the relative sensitivity of 147 hPa radiance to CO at 147 hPa. The residual radiance calculated from the retrieved temperature and mixing ratios is consistent with the measured residual radiance (note that the retrieval at this pressure uses only the channels indicated by the green curve in Figure 6b).

[15] There are channels which deviate from the expected lineshape. Channels near −500 MHz measure a ozone line that is saturated, i.e., sensitive only to atmospheric temperature not to mixing ratios. Channels at line center are sensitive to the large CO mixing ratios in the mesosphere, and the channels at +50 MHz are affected by a weak vibrational line of ozone.

[16] The residual radiance is robust against changes in the regression set: similar results were seen using linear fits calculated using 26 August 2004 radiances in the 30 August 2004 calculations, and vice versa. As a control, the residual radiances were calculated between separate sub-regions of the tropical Pacific, split north-south, or east-west. These residual radiances are close to zero.

[17] The calculation of residual radiance can be applied to individual profiles to give maps of '147 hPa CO radiance' for the tropical troposphere. (The analysis, using the Pacific upper troposphere as the control, precludes the use of the residual radiance outside the tropics.) Values of this radiance, averaged over channels 1–7, 16–21 are mapped in Figure 7. There is excellent agreement, as there should be, between the retrieved 147 hPa CO and the 'CO radiance'.

5. Summary

[18] EOS MLS is producing daily global measurements of carbon monoxide in the atmosphere from ~8 to ~80 km.

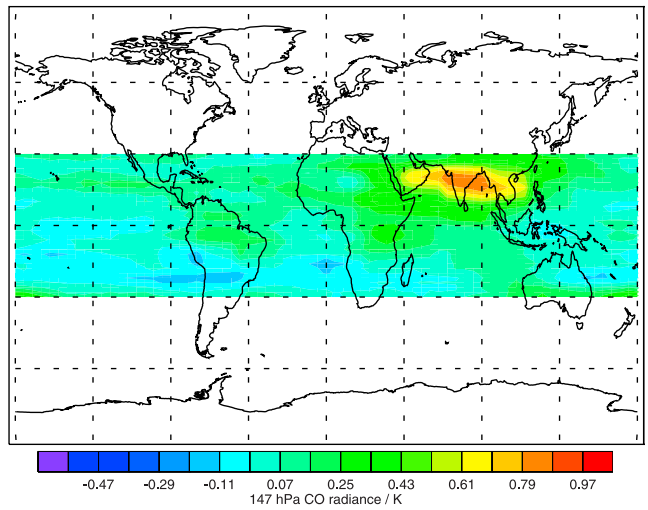

Figure 7. Tropical 147 hPa CO radiance measured by MLS for 30 August 2004. The specific analysis used to derive this radiance is only valid in the tropical troposphere. Range in values corresponds approximately to 0–180 ppbv retrieved CO.

Descent of CO-rich mesospheric air into the north polar stratosphere has been observed in winter 2004–2005, with descent rates up to 21 K/day. A large plume of CO was observed in the upper troposphere over south Asia during August–September 2004, with mixing ratios reaching 180 ppbv. The radiance signal due to this enhanced CO in the upper troposphere has been demonstrated.

[19] **Acknowledgments.** MJF is supported by the UK Natural Environment Research Council. Work at the Jet Propulsion Laboratory, California Institute of Technology was done under contract with the National Aeronautics and Space Administration.

References

Allen, D. R., et al. (1999), Observations of middle atmosphere CO from the UARS ISAMS during the early northern winter 1991/1992, *J. Atmos. Sci.*, *56*, 563–583.

Kar, J., et al. (2004), Evidence of vertical transport of carbon monoxide from Measurements of Pollution in the Troposphere (MOPITT), *Geophys. Res. Lett.*, *31*(23), L23105, doi:10.1029/2004GL021128.

Li, Q., et al. (2005), Convective outflow of South Asian pollution: A global CTM simulation compared with EOS MLS observations, *Geophys. Res. Lett.*, *32*, L14826, doi:10.1029/2005GL022762.

Manney, G. L., et al. (1999), Polar vortex dynamics during spring and fall diagnosed using trace gas observations from the Atmospheric Trace Molecule Spectroscopy instrument, *J. Geophys. Res.*, *104*, 18,841–18,866.

Waters, J. W., et al. (1999), The UARS and EOS Microwave Limb Sounder (MLS) experiments, *J. Atmos. Sci.*, *56*, 194–218.

M. J. Filipiak and R. S. Harwood, Institute of Atmospheric and Environmental Science, School of GeoSciences, University of Edinburgh, Crew Building, The King's Buildings, Mayfield Road, Edinburgh EH9 3JN, UK. (mjf@met.ed.ac.uk)

J. H. Jiang, Q. Li, N. J. Livesey, G. L. Manney, W. G. Read, M. J. Schwartz, J. W. Waters, and D. L. Wu, Jet Propulsion Laboratory, California Institute of Technology, Mail Stop 183-701, 4800 Oak Grove Drive, Pasadena, CA 91109–8099, USA.